ГЕОМАГНЕТИЗМ И АЭРОНОМИЯ

Том 34 1994 № 6

UDK 550.388.8./550.385.4

K. Kauristie, T. I. Pulkkinen and R. J. Pellinen

DYNAMICS OF THE AURORAL OVAL DURING MODERATE SUBSTORMS

Behaviour of the auroral oval during one isolated substorm (15 December, 1982) is studied using DE-1 UV images, DE-2 particle data, and ASC recordings from Kilpisjarvi and Muonio. The observed oval is compared with the statistical oval determined by Feldstein and Starkov. Their model seems to be quite representative during the growth phase but it fails to describe the morning sector widening during the recovery phase. We present initial results of a statistical study concerning the oval boundary movements during moderate magnetic substorms. The study is based on satellite particle data. We divide substorm activity into two categories: $100 < AE < 500$ and $500 < AE < 1000$. Very strong substorms are not included, as the AE station chain cannot record them properly. Three substorm phases (growth, expansion, and recovery) are determined from the AE-index. Comparison between our preliminary results and the statistical model developed by Spiro et al. shows that the shape and size of the oval depend significantly on the substorm phase, not only on the level of magnetic activity. Hence the statistical oval models presented earlier in the literature do not adequately represent the oval during all substorm phases.

1. Introduction

The dynamics and morphology of the auroral oval during magnetic substorms gives us valuable information abour processes going on in the whole magnetosphere. In some cases the global behaviour of the oval can be followed from satellite images, but often only data from local ground-based instruments (like magnetometers and all-sky cameras) are available [1]. Hence a global oval model which could be combined with local observations would often be useful.

Observations show that the size of the auroral oval depends mainly on IMF B_z and substorm activity (for a review, see [2]). Even though IMF B_z and substorms are related, they affect the oval in different ways. Whereas substorms strongly affect the location of the poleward boundary, the IMF B_z more clearly controls the size of the visual oval (i. e., the equatorward boundary). The solar wind speed (V) does not vary as much as IMF B_z, but it affects the oval size through solar wind motional electric field (VB_z): The strength of the sunward magnetospheric convection affects the equatorward boundary of the oval [2].

Some statistical models for the oval have already been developed in the literature (cf. [3] and [4]) but they are not suitable for substorm studies since the oval shape and location depend only on the level of magnetic activity, which is characterized by the magnetic indices (like Q or AE). However, the shape of the oval is different e. g. during the growth phase and the recovery phase even though magnetic activity is at the same level [5].

2. Behaviour of the oval during one isolated substorm

On 15 December, 1981 1930—2230 UT the magnetometer stations in Northern Finland and Scandinavia recorded a very isolated substorm. The behaviour of the IMF B_z clearly controls the substorm process (data not shown): It turns southwards

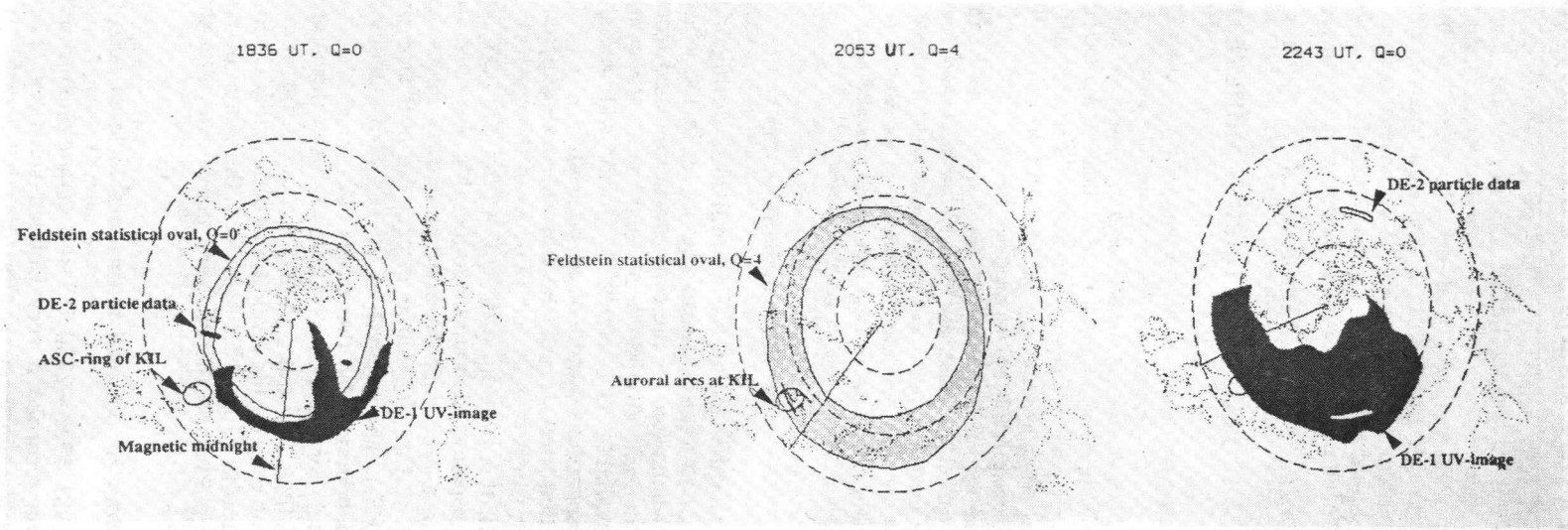

Fig. 1. Substorm on 15 December, 1981. Left panel: Growth phase (1836 UT), *DE*-2 particle data shows precipitating electrons with energies >1 keV. Middle panel: Expansion phase (2053 UT), auroral expansion at KIL. Right panel: Recovery phase (2243 UT), De-2 data shows the boundaries of the diffuse oval

at 1820 UT (the UT scale of ISEE-3 recordings has been shifted later by one hour) and about 40 minutes later the AE-index starts to increase. The first reddish auroral arc (at an altitude of more than 150 km) appears at the northern sky of Kilpisjarvi (KIL, 69.0 N, 20.8 E) at 1940 UT and during the growth phase it moves steadily southwards and brightens. The onset occurs at 2036 UT and during the expansion phase discrete arcs expand polewards forming the head of a westward travelling surge. The surge crosses the zenith of KIL at 2049 UT after which IMF B_z turns gradually back to north. Consequently the substorm starts to decay and the AE-index returns back to its quiet level.

DE-1 was at its perigee position during the actual substorm. Hence we can determine the location of the oval only at the beginning and at the end of the substorm sequence. During the substorm we estimated the locations of the oval boundaries by interpolating between the UV-images and by using DE-2 particle data [6] and ASC-recordings from KIL and Muonio (68.0 N, 23.6 E). Fig. 1 shows the auroral distributions during substorm growth, expansion, and recovery. The left panel shows the auroras recorded by the DE-1 imager, and the statistical oval of Feldstein and Starkov [3] for Q = 0 is shown for reference. During the expansion phase (centre panel) no global data are available, but the ASC-observations fit well within the Feldstein and Starkov oval for Q = 4. However, during the substorm recovery phase (right panel), it is clear that although the Q-index at Sodankyla (67.4 N, 26.6 E) has decreased back to zero, the oval is still very wide, and the statistical representation is not adequate.

3. Statistical data analysis

Our statistical oval model for substorm periods is based on recordings of the TED (Total Energy Detector) instruments on TIROS-N, NOAA-6, and NOAA-7 satellites. TED determines total energy flux of electrons and ions mapped to the altitude of 120 km [7]. In this study the oval is defined to be the area with total flux mainly above 1 erg/s*cm^2. UT times of the oval boundary crossings were saved and the corresponding substorm phases were determined from the AE-index. The substorms studied (about 120) are from periods April-May 1986, August 1979, April-May 1980, and November 1981.

The data were binned in four categories: Growth, onset, expansion and recovery. As finding the exact onset moment from an AE-curve is not always possible we determine and "onset phase" during which the onset most probably happens. Usually this phase is very short (some tens of minutes) and hence its statistical analysis is not yet possible with our limited initial data set.

Data points were divided into two bins according to magnetic activity. AE values for two hours before the considered moment were taken into account. If max(AE) was below 500 nT the data point was stored into the moderate activity bin and if max(AE) exceeded 500 nT data point was stored into strong activity bin. Data points with AE > 1000 nT were ignored because then the oval is mostly beyond the reach of the AE station chain (i. e., at too low latitudes) and hence determining substorm phases from the AE-index is much more difficult.

4. Moderate substorm activity

The left panel of Fig. 2 shows the movements of the oval boundaries during moderate isolated substorms. The ovals have been cut open at the noon meridian to make the differences between the three substorm phases more clearly visible. The curves are 4th order polynomials fitted to two-hour mean values of the data points. Amount of points used to create these curves varies from 100 to 128. The growth phase oval seems to be close to the quiet time oval, because a large part of the data points represent the beginning of the growth phase (after a two-hour quiet time period) when the polar cap has not yet expanded. The increase in the

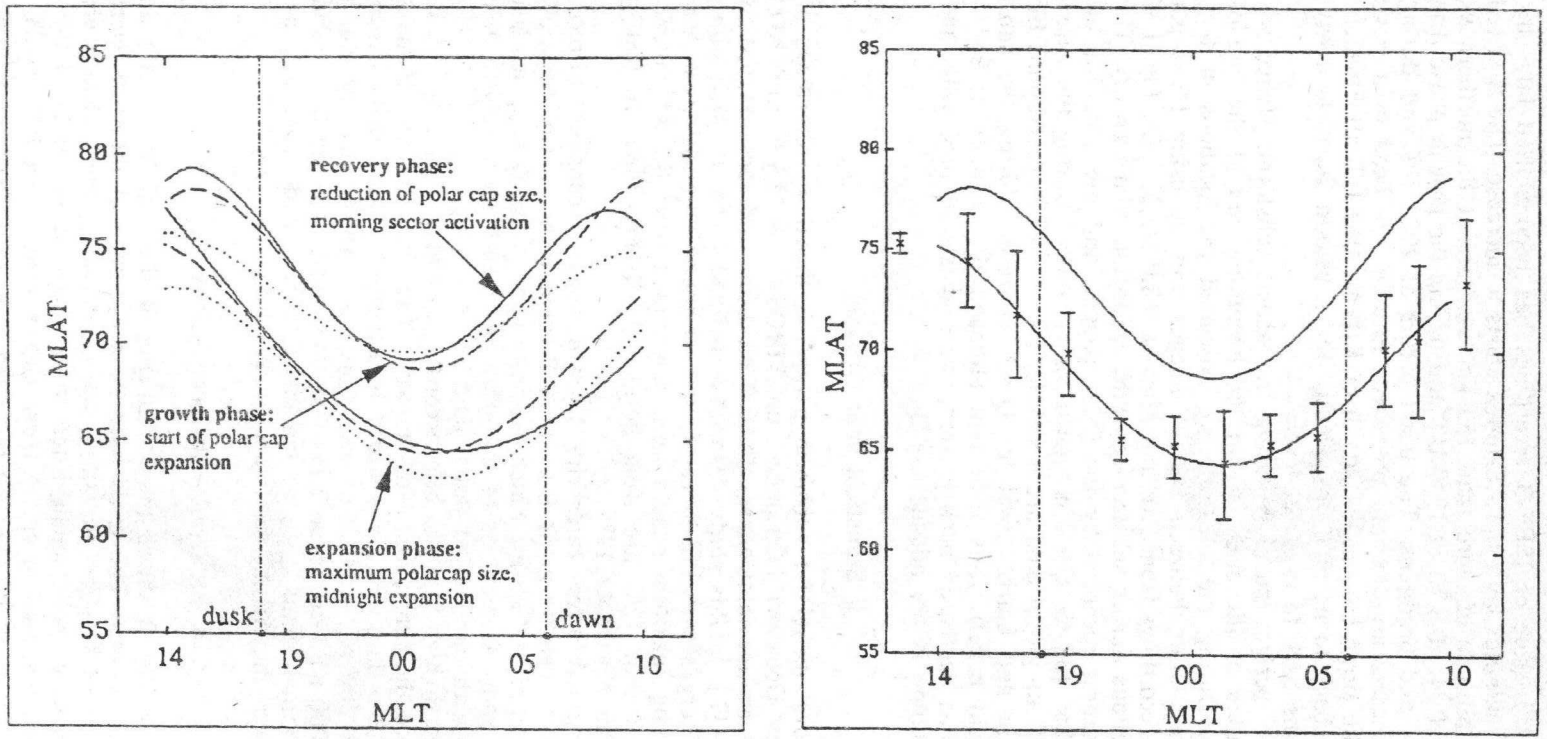

Fig. 2. Left panel: Movements of the oval during moderate, isolated substorms. Right panel: Scattering of the datapoints determining the equatorward boundary of the growth phase oval. The error bars are standard deviations of the points in each two-hour bin (see text)

Table 1

Rough estimations (see text) of polar cap areas for oval models shown in Figs 2 and 3

	Moderate substorms ($\cdot 10^7$ km^2)	Strong substorms ($\cdot 10^7$ km^2)	(A(Str)-A(Mod))/A(Mod) (%)
Expansion	1.01	1.06	5
Recovery	0.81	0.79	−2
A(Rec)/A(Exp) (%)	81	75	

polar cap size can be seen more clearly in the expansion phase oval, which also shows the midnight sector widening. The morning sector of the recovery phase oval is wide as expected (cf. Fig. 1, right panel). The evening sector resembles that of the growth phase (quiet) oval as the magnetic activity has ceased there. The size of the polar cap during the recovery phase has reduced from that during the expansion phase by almost 20% (cf. Table 1). The right panel of Fig. 2 depicts scattering of the data points (amount 124) determining the equatorward boundary of the growth phase oval.

5. Comparison of moderate and strong substorm activity

In order to get enough data points (i. e., about 100) for strong activity oval model we had to combine two data sets in which MLT and MLAT were determined using different methods. However, the possible systematic error between these data sets is small, much less than the random scattering of the points. Fig. 3 shows a comparison between strong and moderate activity ovals during the expansion and recovery phases. The amount of points used to create the strong activity curves varies from 102 to 158. Growth phase analysis has been omitted as there were not enough points for a reliable fit. As expected, the strong activity ovals are much wider and at lower latitudes than the moderate activity ovals.

During the expansion phase the size of the strong activity polar cap is larger than that of the moderate activity. We have estimated the polar cap areas of our oval models roughly by using the discrete points (two-hour means) used in Figs 2 and 3. The results are shown in Table 1. Note that during the recovery phase the area is slightly smaller for strong activity than for moderate activity. This may reflect either stronger reconnection in the tail during large substorms, or it could be an artefact of the relatively small data set.

6. Discussion and conclusions

We presented preliminary results of a statistical study of the dynamics of the auroral oval during moderate substorms. Even with this limited data set qualitative differences in the oval shape during different substorm phases can clearly be seen: The growth phase model (for moderate isolated substorms) shows a relatively quiet but slightly expanded oval. The expansion phase model shows the maximumsize oval, and the recovery phase model shows the features typically associated with late phases of the substorm (wide morning sector oval, reduced polar cap size).

As TED instruments on TIROS/NOAA satellites record energies below 20 keV, our model describes the changes in the discrete oval. According to Galperin and Feldstein [8] the poleward boundary of the discrete oval seems to correspond to the boundary between the central plasma sheet (CPS) and the boundary plasma sheet (BPS) in magnetosphere. The equatorward boundary maps to the inner edge of the CPS. Galperin and Feldstein established their view by comparing CPS plasma parameters with the parameters of plasma causing the oval luminosity. In addition,

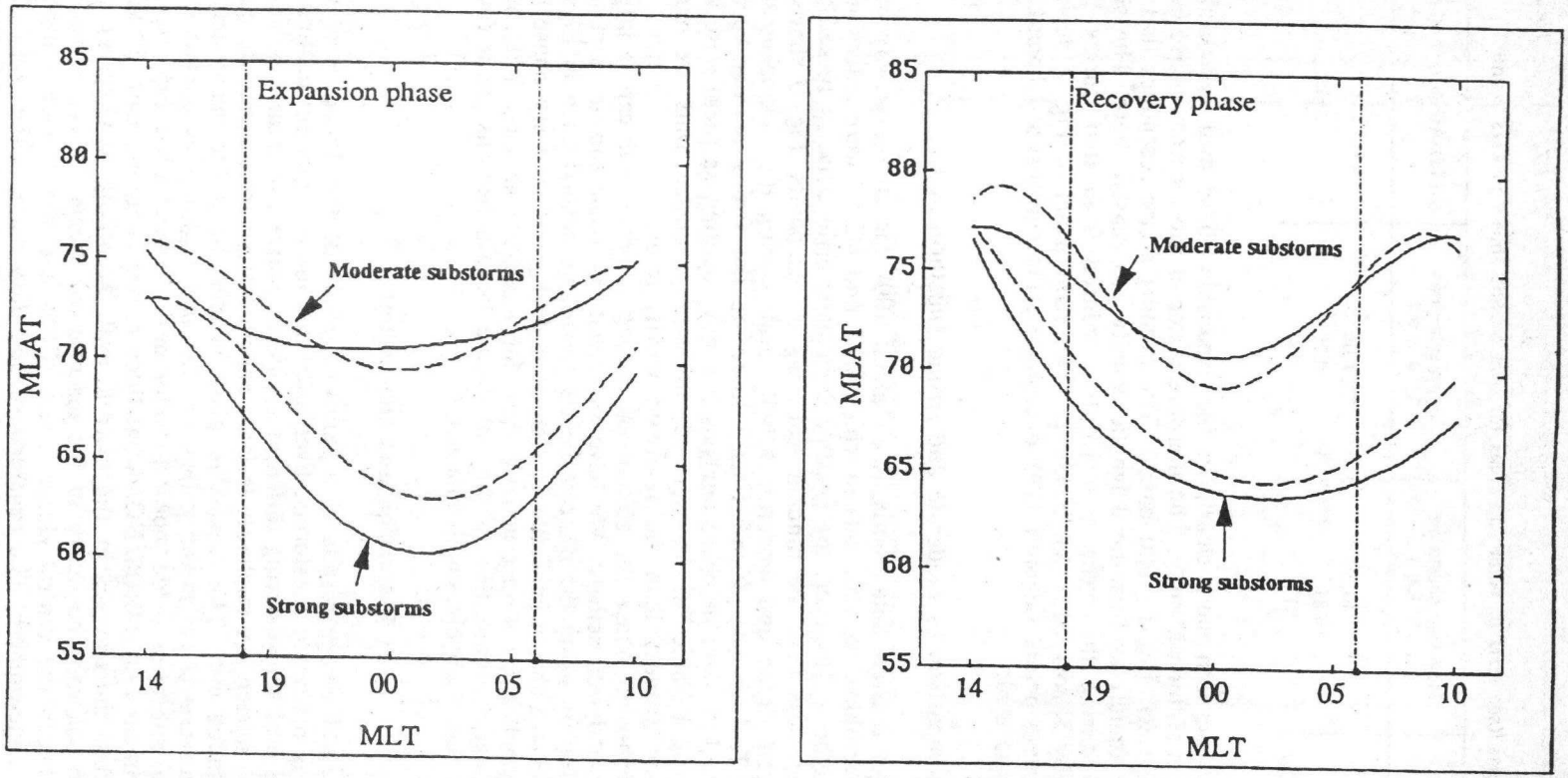

Fig. 3. Comparison between moderate (dashed line) and strong (solid line) substorms

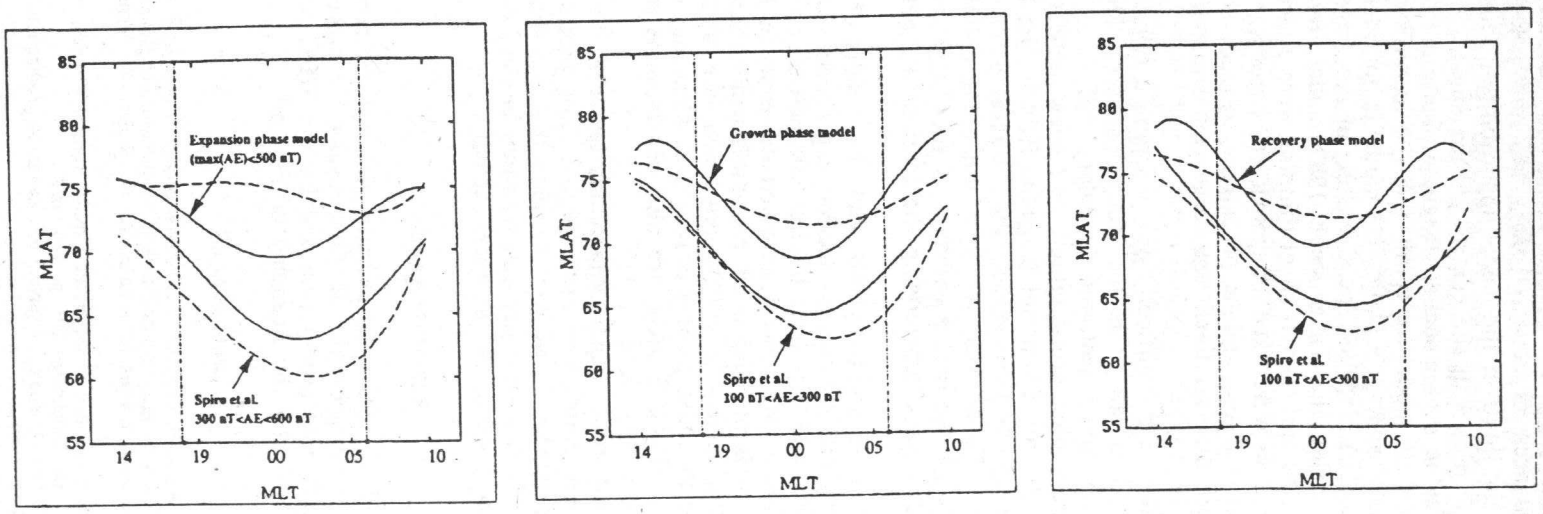

Fig. 4. Comparison between our results for moderate substorms (solid line) and the oval models for $100 < AE < 300$ and $300 < AE < 600$ of Spiro et al. (dashed line)

the magnetic field models of Tsyganenko [9] map the equatorward boundary of the oval to radial distances of $R \approx 5-10 R_E$, and the poleward boundary to $R \approx 40-70 R_E$ (i. e., to the limits of the model applicability). This is also consistent with relating the discrete oval with the central plasma sheet.

Before we can utilise the oval model in magnetospheric substorm research, we need a reliable magnetic field model for connecting the features of the auroral oval to certain regions in magnetosphere. A static field model is not adequate for substorm studies. Pulkkinen et al. [10] modelled the stretching of the magnetotail during the substorm growth phase using the Tsyganenko 1989 model, to which temporally evolving near-Earth currents and current sheet thinning were added. The parameters controlling these modifications were fixed using spacecraft observations. In the events they studied they found that the regions of extreme current sheet thinning and chaotic electron motion (in the near-Earth equatorial plane) mapped into the regions of brightening auroras.

Sergeev et al. [11] discuss the difficulty of developing a reliable magnetic index which describes best the situation in the magnetosphere. They defined from NOAA/TIROS data a so called isotropic boundary (IB, i. e., the equatorward boundary of the isotropic proton precipitation) and show that the location of the IB is strongly controlled by the equatorial magnetic field in the tail. Hence, when constructing and using magnetic field models they suggest using the IB instead of ground-based indices (like K_p or AE). As an example the authors show how the IB can be used for choosing the best K_p-version of the Tsyganenko 1989 models. IB could be a useful index for characterising the level of magnetic activity in our oval study, too.

In Fig. 4 our model ovals are compared with the results of Spiro et al [4]. They have used data from the low energy electron experiments on the Atmosphere Explorer C and D satellites and they have binned data points according to invariant latitude, MLT, and AE-index. We have determined the ovals in Fig. 4. from their Table 2. In general, the ovals of Spiro et al. are much wider than the ovals in our model. One reason for this is that they have not taken into account the substorm phase preceding the time the data point was recorded. Consequently, in their bins $100 < AE < 300$ and $300 < AE < 600$ there are also observations made after strong substorms when the oval is very wide.

Even though we cannot make exact comparisons between the curves in Fig. 4 (the ovals of Spiro et al. are determined using only electron precipitation data while in our data also ions are included), we can conclude that the shape of the auroral oval varies during substorms in such a way that it cannot be described with statistical models depending only on level of the magnetic activity.

Acknowledgements

We would like to thank R. Dyson (University of Iowa) for processing the DE-1 imager data. We thank V. Sergeev and B. Gvosdevsky for processing the NOAA particle data that originally was kindly provided by the WDC-A in Boulder. The work of K. K. was supported by the Academy of Finland.

REFERENCES

1. *Pellinen R. J., O. A. Aulamo, J. D. Craven, L. A. Frank, and J. S. Murphee.* On the use of topside auroral image together with various ground-based data to study local and global auroral development. Progress in Atmospheric Physics. Editors R. Rodrigo et al., Kluwer Academic Publishers. p. 197. 1988.
2. *Siscoe G. L.* What determines the size of the auroral oval? Auroral Physics, edited by C.-I. Meng, M. J. Rycroft and L. A. Frank. Cambridge UP. p. 159. 1991.
3. *Feldstein Y. I. and G. V. Starkov.* Dynamics of auroral belt and polar geomagnetic disturbances//Planet. Space Sci. 15, No. 2, p. 209. 1967.
4. *Spiro R. W., P. H. Reiff and L. J. Maher, Jr.* Precipitating electron energy flux and auroral zone conductances — an empirical model. Journal of Geophysical Research. 87, A10, p. 8215. 1982.

5. *Opgenoorth H. J., M. A. L. Persson, T. I. Pulkkinen, and R. J. Pellinen.* The Recovery Phase o Magnetospheric Substorms and its Association with Morning-Sector Aurora. Journal of Geophysica Research, in press. 1993.
6. *Sharber J. R. and J. D. Winningham.* Dynamics Explorer-2 measurements during and isolated aurora substorm. In Proceedings of the Third Finnish-American Auroral Workshop. October 14-18, 1985, ir Sodankyla, Finland. Editors E. Turunen and E. Kataja. Report No. 45. The Finnish Academy o Science and Letters Sodankyla Geophysical Observatory.
7. *Hill V. J., D. S. Evans and H. H. Sauer.* TIROS/NOAA satellites space environment monitor archive tape documentation. NOAA Technical Memorandum ERL SEL-71. 1985.
8. *Galperin Yu. I. and Ya. I. Feldstein.* Auroral luminosity and its relationship to magnetospheric plasma domains. Auroral Physics, edited by C.-I. Meng, M. J. Rycroft and L. A. Frank. Cambridge UP. p. 207. 1991.
9. *Tsyganenko N. A.* Magnetospheric magnetic field model with a warped tail current sheet. Planet. Space Sci. 37, No. 1, p. 5. 1989.
10. *Pulkkinen T. I., D. N. Baker, R. J. Pellinen, J. Büchner, H. E. J. Koskinen, R. E. Lopez, R. L. Dyson, and L. A. Frank.* Particle Scattering and Current Sheet Stability in the Geomagnetic Tail During the Substorm Growth Phase. Journal of Geophysical Research, 97, No. A12, p. 19283. 1992.
11. *Sergeev V. A., M. Malkov, and K. Mursula.* Testing the Isotropic Boundary Algorithm Method to Evaluate the Magnetic Field Configuration in the Tail. Journal of Geophysical Research, 98. No. A5, p. 7609. 1993.

Finnish Meteorological Institute,
Department of Geophysics